

QUANTITATIVE SIMULATION OF NIRS-930 CYCLOTRON

V.L. Smirnov, S.B. Vorozhtsov, JINR, Dubna, Russia

A. Goto, S. Hojo, T. Honma, K. Katagiri, NIRS, 4-9-1 Anagawa, Inage, Chiba, Japan

Abstract

The results of the computer modelling of the structural elements of the NIRS-930 cyclotron operational at the National Institute of Radiological Sciences (Chiba, Japan) are presented. The integrated approach to modelling of the cyclotron, including calculation of electromagnetic fields of the structural elements and beam dynamics simulations is described. A computer model of the cyclotron was constructed. Electric and magnetic field distributions and mechanical structures were converted to the beam dynamics code for simulations, in which particle losses on the surfaces of the system elements were estimated. The existing data on the axial injection, magnetic, acceleration and extraction systems of the cyclotron and beam parameter measurements are used for calibration of the simulations. New acceleration regimes could be formulated with the help of the constructed computer model of the machine.

INTRODUCTION

The main cyclotron facility at the National Institute of Radiological Science (NIRS) is the NIRS-930 cyclotron [1]. The facility has been used for production of radioisotopes and short-lived radio-pharmaceuticals for PET, physics research, development of particle detectors in space, etc.

The main regime for acceleration of 30 MeV protons (p30 in Fig. 1) was considered for the construction of the computer model of the cyclotron and demonstration calculations with its help.

The major issues in the computer modelling of the cyclotron are optimization of the existing acceleration regimes (Fig. 1) to increase the beam intensity and to improve the beam quality. Also, retesting of the ion acceleration at the 3rd RF harmonics could be attempted. Some modifications of the cyclotron acceleration regime parameters and its structural elements are expected for broadening the cyclotron capacity.

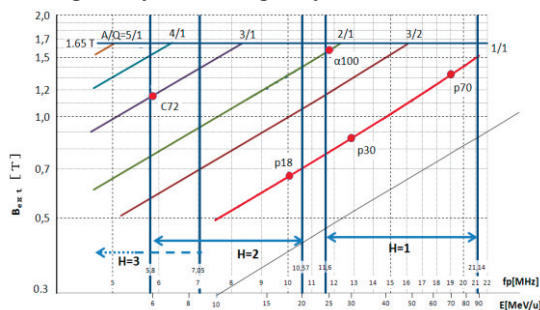


Figure 1: Operation diagram: points – experimental regimes (C72 – 72 MeV $^{12}\text{C}^{4+}$, $\alpha 100$ – 100 MeV $^4\text{He}^{2+}$, p18, p30, p70 – 18, 30, 70 MeV protons), H – RF harmonic. H=3 regime is still waiting to be explored.

ELECTROMAGNETIC FIELDS

Computer modelling of the structural elements of the NIRS-930 cyclotron is an essential part of the integrated approach to the modelling of the cyclotron as a whole [2]. The corresponding computer model of the facility is presented in Fig. 2. The electric and the magnetic field distributions obtained with this model and the mechanical structures were converted to the beam dynamics code for simulations.

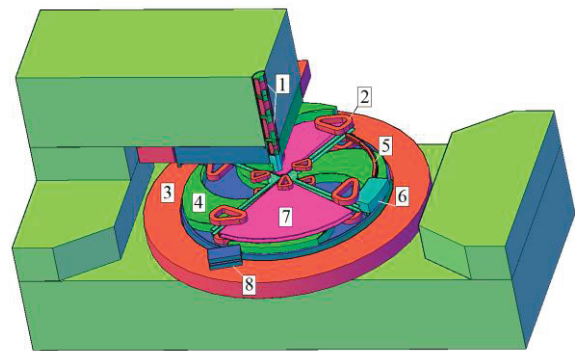


Figure 2: Computer model of the cyclotron: 1 – glazer lenses, 2 – harmonic coils, 3 – main coil, 4 – sector, 5 – electrostatic deflector, 6 – magnetic channel, 7 – dee, 8 – gradient corrector.

Our simulations started from the point 200 mm upstream of the buncher. The main structure elements used in the three-dimensional electromagnetic field generation and in the beam dynamics analysis are a single-gap buncher and four glazer lenses. The single-gap buncher has a five mm gap between the RF electrodes and a grid with transparency ~98 %.

The four glazer lenses downstream of the buncher are used to match the beam with the cyclotron centre acceptance. The lenses have the same structure, but small difference in geometrical size.

The magnetic field of the main magnet was calculated by the Opera3D [3] software. The cyclotron magnet has four spiral sectors for shaping the magnetic fields in the median plane of the machine and 12 pairs of trim coils that are used for fine adjustment of the field to the required isochronous performance. Eight pairs of harmonic coils (four in the central region and four near the extraction radius) serve for correcting the so-called “natural” 1st harmonics in the expansion of the magnetic field and for introducing a field bump in the extraction region to increase turn separation between the neighbouring orbits there.

The existing magnetic field measurements for the so-called “iron” field (only the main coil was on, and all trim

coils were with zero current) permit the calculated mean magnetic field dependence on the radius to be compared with the experimental data. Field comparison for the main coil current of 450 A, which is close to the one in the acceleration regime was made. There was good agreement between them (deviation of only several Gauss) except for the central region. The deviation could be explained by the existing uncertainty in the knowledge of the magnetic property of the magnet core and by some possible differences in the details of the model and the real magnet geometry.

The next step was calculation of the trim coil field contributions, which were apparently dependent on the level of the magnet magnetization. Twelve pairs of circular trim coils are located on the surface of the sectors. There is good agreement between the calculated and measured curves with somewhat larger deviations in the central region of the machine.

An overall comparison of the calculations and measurements for the “iron” field and the trim coil contributions proves that the computer model is very close to the real situation. This means that for the given set of the main and trim coil currents the computer model should produce a sufficiently realistic field distribution without checking it by the measurements.

Given spiral inflector parameters – magnetic and electric radius – a computer model of the device can be prepared. To this end, the real procedure of drilling the gap between the inflector electrodes should be simulated at the computer, which comprises simulation of the motion of the drilling tool along the inflector axis and its rotation around this axis [4]. The size of the tool corresponds to the air gap between the electrodes. The trajectory of the tool follows the pre-calculated central line between the inflector electrodes. The thus obtained model of the inflector was used for spatial electrostatic field calculation inside and around the inflector.

The acceleration system of the cyclotron consists of two 86° dee electrodes. The constructed computer model permits the spatial distribution of the electrical field to be evaluated by the Opera3D software (electrostatic version). Preliminary analysis of the RF structure under consideration shows that this approximation is sufficiently good.

The extraction system of the cyclotron consists of an electrostatic deflector, an active magnetic channel and a passive gradient corrector of the main cyclotron field in the extraction region.

The septum of the deflector is subdivided into two parts with the 1st part (pre-septum) having a V-shape cut along the beam and being insulated from the earth potential. The “floating septum system”, which is able to read out the beam current on the pre-septum, was developed in order to preserve it from the thermal damage due to the irregular beam hitting.

The magnetic channel is composed of four coils made with hollow conductors [5]. The passive gradient corrector (no coils) is located near the outlet window of the cyclotron vacuum chamber.

The constructed computer models of the extraction system elements described above were used for generation of their electromagnetic field distributions used afterwards in the beam dynamics analysis program.

BEAM DYNAMICS

Similar to the testing and calibration of the computer model of the cyclotron for generation of the electromagnetic field, the acceleration regime for 30 MeV protons was also used for the beam dynamics analysis. In this regime the maximum beam transmission efficiency was realized experimentally. There are data on beam intensities measured by probes at various locations in the machine, which can be compared to the corresponding simulation results.

Initial adjustment of the parameters of the beam dynamics calculations was performed with the help of the reference particle tracing. Here the adjustment of the system parameters means shifting of the puller along the 1st dee and the rotation of the inflector around its axis. Also, the inflector axial shift is used to suppress axial oscillations of the reference particle. The orbit study was performed with the existing configuration, where the cyclotron parameters were set to acceleration of protons with the energy of 30 MeV in the daily operation.

Analysis of the RF phase excursion in acceleration shows that the deviation of the phase from the optimal one (with maximum energy gain per turn) is rather small, which is a manifestation of the field shaping be very close to the isochronous one. The RF phase calculation results also agree with the experimental phase probe reading for this regime (see Fig. 3).

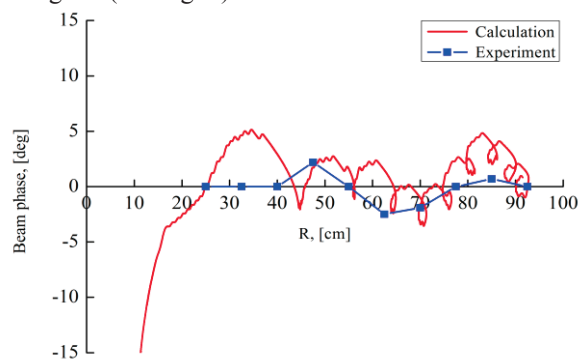


Figure 3: Calculated RF phase excursion to compare to the reading of the phase probe.

To start estimation of beam transmission through various units of the cyclotron, some initial distribution of particles with 10^5 macro-particles in the plane 200 mm upstream of the buncher was prepared. Transverse emittances were taken to be 150π -mm-mrad and the energy spread in the beam was set to ± 1 eV. Macro-particles in the beam were traced through the cyclotron with allowance for the space charge effects. The injected beam intensity was 130 μ A.

In the simulations, the buncher voltage was 260 V, which ensured longitudinal focus in the median plane. With the experimental settings of the glazer lenses in the

axial injection line the calculated beam transverse dimensions fitted to the inflector gap.

Beam dynamics analysis showed that the majority of the particle losses took place on the inflector, the inflector case and the dee posts (see Fig. 4). There were also some (~2-3 %) particle losses inside the glazer lens nearest to the median plane of the cyclotron. The total particle losses are 69 % of the incoming beam.

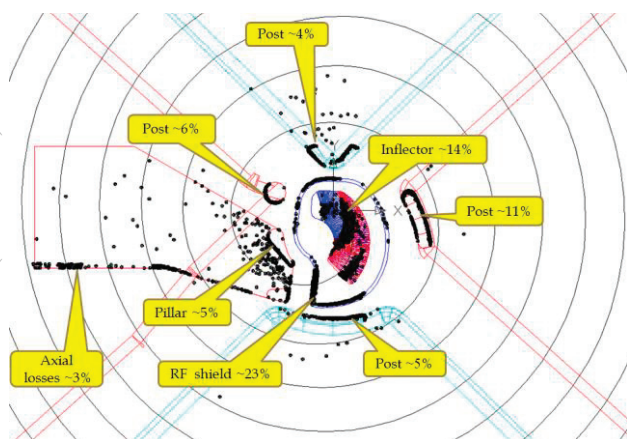


Figure 4: Distribution of the particle losses in the central region. Black dots are location of the lost particles

The inflector voltage was adjusted to minimize coherent axial oscillation of the beam in the central region. This ensures rather small axial emittance at the end of the acceleration process, i.e. at the deflector entrance. The radial emittance is defined by the existing radial oscillation of particles and also by the energy spread in the bunch. The longitudinal length of the beam is $\pm 25^\circ \text{RF}$ since the lagging ions were lost in the central region of the cyclotron. Some ions returned to the central region and got lost there (~11 %).

The calculations show that the beam extraction efficiency is ~39 %. As expected, almost all particle losses take place on the septum of the electrostatic deflector. The multiturn extraction (about nine turns) appears to be a consequence of insufficient turn separation under rather large beam radial emittance at the entrance of the deflector.

A comparison of the beam intensity measurements with the calculation permits one to assess how much the constructed computer model agrees with reality. Table 1 shows the results of this comparison, namely, the beam transmission through various units of the machine. Here,

Table 1: Transmission, %.

Range	Calculation		Experiment
	No space charge effects	Space charge effects included.	
Central region	35	31	29
Acceleration	92	89	89
Extraction	43	39	49
Total	14	11	12

the transmission is defined as a ratio of the beam current at the exit and at the entrance of the given unit.

Some impression of the extracted beam quality can be obtained from Fig. 5. In the figure, a rather long “tail” is seen on the left side of the particle distributions. In some cases this “tail” transforms to a satellite beam on the left of the histograms.

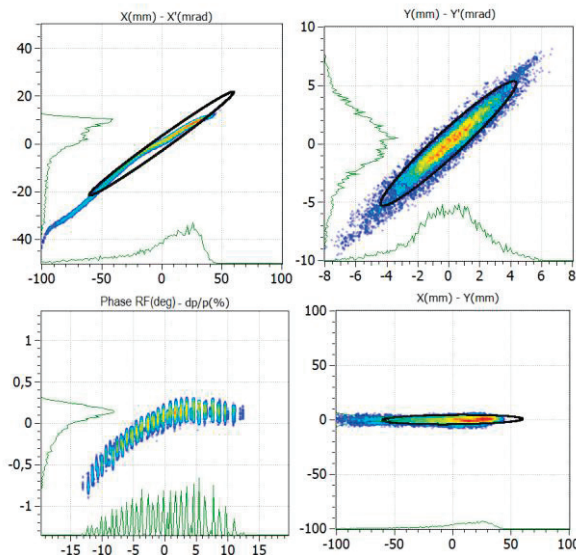


Figure 5: Beam emittances at the outlet window.

Objectives for the future to be studied hereafter are:

- Optimization of the operational parameters for typical beams covering the whole performance area of the NIRS-930 cyclotron (see Fig. 1). Improvement of transmission through the cyclotron and beam quality are expected from the optimization.
- Retesting the formerly designed central region for H=3 and its redesigning, if necessary.

REFERENCES

- [1] A. Sugiura, et al., "Status Report of NIRS Cyclotron Facility (NIRS-930, HM-18)", Proceedings of the 8th Annual Meeting of Particle Accelerator Society of Japan (August 1-3, 2011, Tsukuba, Japan).
- [2] B. Wang, H. Hao, S.B. Vorozhtsov, V.L. Smirnov, Q. Yao, J. Zhang, M. Song, H. Zhao, "Computer Design of a Compact Cyclotron", Physics of Particles and Nuclear Letters, 2012, Vol. 9, No. 3, pp. 288–298.
- [3] OPERA/TOSCA Reference Manual. Vector Fields Limited. Oxford, OX5 1JE, England.
- [4] S. B. Vorozhtsov, A. S. Vorozhtsov, S. Watanabe, S. Kubono, A. Goto, "Computation of Cyclotron Electromagnetic Fields", Nuclear Science, IEEE Transactions on, vol. 58, №. 3, pp.1181-1187, 2011.
- [5] S. Hojo, et al., "Design Study of Magnetic Channel at NIRS-AVF930", Proc. 19th Int. Conf. on Cyclotrons and their Applications, 2010.